Hindawi Publishing Corporation
Mathematical Problems in Engineering
Volume 2015, Article ID 103809, 11 pages
http://dx.doi.org/10.1155/2015/103809

Research Article

A Reduced-Order Model for Complex Modes of Brake Squeal Model and Its Application to a Flexible Pin-on-Disc System

Lijun Zhang,[1,2] Jun Wu,[1,2] and Dejian Meng[1,2]

[1]*School of Automotive Engineering, Tongji University, Shanghai 201804, China*
[2]*Collaborative Innovation Center for Intelligent New Energy Vehicle, Tongji University, Shanghai 201804, China*

Correspondence should be addressed to Lijun Zhang; tjedu_zhanglijun@tongji.edu.cn

Received 16 March 2015; Accepted 13 May 2015

Academic Editor: Roman Lewandowski

Brake squeal is often analytically studied by a complex eigenvalue analysis of linearized models of the brake assembly that is usually quite large. In this paper, a method for determining those frequencies having the most effect on the pair of coupling frequencies that saves much time is put forward and a reduced-order model is presented based on the complex modes theory. The reduced-order model is proved to be effective when applied to a flexible pin-on-disc system; even damping and nonlinearity are taken into consideration. This reduced-order model can predict the onset of squeal as well as the squeal frequency with sufficient accuracy and largely reduced amount of calculation and gives us a practical guide to perform design optimization in order to reduce brake squeal.

1. Introduction

The problem of disc brake squeal has long been a major concern for the automobile industry. During the past few decades, brake squeal has been studied thoroughly by both theoretical and experimental approaches. Till now, four main frictional squeal mechanisms are highlighted; they are mode coupling instability theory, negative friction-velocity slope instability theory, sprag-slip motion theory, and stick-slip motion theory [1]. Among these theories, mode coupling instability theory is most widely accepted by the academic world, many researches have shown that mode coupling instability frequency is nearly consistent with the squeal frequency [2–5], which suggests a complex modal analysis of brake system models as a tool of investigation on squeal and this method is widely used in industry with the help of finite element software to predict the squeal frequency.

Typically, the order of the modal-based brake system model is quite large, which creates a formidable task of studying coupling among a large number of modes for the prediction of the onset of squeal and the instability frequency. However, it can be found that mode coupling is the coupling between a single pair of modes or coalescence of two eigenfrequencies of the system and a great majority of modes have little influence on the coupling between these two modes [6–10], so many scholars, such as Ouyang and Huang, have put forward their methods to simplify the system so as to predict the onset of squeal or squeal frequencies with largely reduced amount of calculation and sufficient accuracy, which is proved to be effective under certain circumstances. For example, Huang et al. [6] presented a perturbation method for determining the critical friction coefficient for disc brakes based on the eigenvalues and eigenvectors of the elastically coupled system. However, this method can only be effective under the condition of real mode and other modes have little effect on the two coupling modes. What is more, it does not work well when used to predict the squeal frequency when friction coefficient is large. Ouyang et al. [7] present a different and more efficient approach based on the receptance of the symmetric system, and the efficiency of this method relies on the knowledge of measured receptances. Unfortunately, these methods can only be applied to real modes. Nevertheless, in many engineering problems such as the system with nonproportional damping, dynamic system under nonconservative forces, analysis of aeroelastic flutter, the system matrices are not real symmetric and may be

complex asymmetric. What is more, when the nonlinearity factors are taken into consideration, the linearized system will be more complicated so as to lead to the failure of these methods. In this case, a new method needs to be developed for the complex modes to simplify the system so as to predict the onset of squeal and squeal frequency with sufficient accuracy. As everyone knows, the matrix perturbation theory [11] is an efficient method when applied to small changes of the structure; Huang's method is a convergent method in spite of inaccuracy in some situation.

In this paper, a method combining the matrix perturbation theory for complex modes with Huang's method is developed to judge those eigenfrequencies having the greatest effect on the two coupling eigenfrequencies, which is time-saving and then a reduced-order method for complex modes system is put forward to predict the onset of squeal and squeal frequency. What is more, this method is applied to a nonlinear flexible pin-on-disc system and accurate results are obtained. This method provides us with an insight into the dependence of propensity to squeal on system parameters and thus performing design optimization.

2. Method to Determine the Influential Eigenfrequencies

2.1. Matrix Perturbation for Complex Modes. The free vibration equations of the linear or linearized systems with N modes are as follows:

$$\ddot{\mathbf{Y}} + \mathbf{C}_1\dot{\mathbf{Y}} + \mathbf{K}_1\mathbf{Y} = \mathbf{0}, \tag{1}$$

where the matrix $\mathbf{C}_1$ is assumed to be complex asymmetric because of, for example, the rotation of the disc and nonlinearity. Similarly, the matrix $\mathbf{K}_1$ is assumed to be complex asymmetric because of, for example, the effect of the nonconservative forces—frictional force.

The governing equations in (1) are mapped into a state space by introducing $\mathbf{z} = \left[\begin{smallmatrix}\mathbf{Y}\\ \dot{\mathbf{Y}}\end{smallmatrix}\right]$; (2) can be derived from (1) as

$$\mathbf{T}_1\dot{\mathbf{z}} + \mathbf{T}_2'\mathbf{z} = \mathbf{0}, \tag{2}$$

where $\mathbf{T}_1 = \mathbf{E}$, $\mathbf{T}_2' = \left[\begin{smallmatrix}\mathbf{O} & -\mathbf{E}\\ \mathbf{K}_1 & \mathbf{C}_1\end{smallmatrix}\right]$.

The eigenvalue problem corresponding to the system in (2) is shown below:

$$\left(\lambda\mathbf{T}_1 + \mathbf{T}_2'\right)\mathbf{U}_r = 0, \tag{3}$$

where λ and $\mathbf{U}_r$ are the eigenvalue and right eigenvector of the system, respectively.

Consider the following power series expansions for $\mathbf{T}_2'$ with respect to the coefficient of friction $\mu = \varepsilon_\mu$:

$$\mathbf{T}_2' = \mathbf{T}_2 + \sum_{k=1}^{n}\varepsilon_\mu^k\mathbf{T}_{2,\varepsilon^k} + \cdots \tag{4}$$

It should be noted that $\mathbf{T}_2$ is the matrix when the components of the system are coupled only by normal stiffness of the lining, or it can be said that there is no friction between components, or the coefficient of friction $\mu = \varepsilon_\mu$ sets to be zero, under which situation the system is chosen to be the unperturbed system.

The eigenvalue problem corresponding to the unperturbed system of (2) is

$$\left(\lambda_i^{(0)}\mathbf{T}_1 + \mathbf{T}_2\right)\mathbf{U}_{ri}^{(0)} = 0, \tag{5}$$

where $\lambda_i^{(0)}$ and $\mathbf{U}_{ri}^{(0)}$ $(i = 1, 2, \ldots, 2N)$ are the eigenvalue and right eigenvector of the unperturbed system, respectively.

The left eigenvalue problem associated with the unperturbed system in (5) is

$$\left(\lambda_i^{(0)}\mathbf{T}_1 + \mathbf{T}_2\right)^T\mathbf{U}_{li}^{(0)} = 0, \tag{6}$$

where $\lambda_i^{(0)}$ and $\mathbf{U}_{li}^{(0)}$ $(i = 1, 2, \ldots, 2N)$ are the eigenvalue and left eigenvector of the unperturbed system, respectively. Note that the eigenvalues in (5) and (6) are the same since the matrixes $-\mathbf{T}_2$ and $-\mathbf{T}_2^T$ have the same $2N$ eigenvalues in the complex domain.

It is assumed that the right and left eigenvectors are normalized to satisfy the biorthogonality condition

$$\mathbf{U}_{ls}^{(0)T}\mathbf{T}_1\mathbf{U}_{ri}^{(0)} = \delta_{is} = \begin{cases}1, & i = s\\ 0, & i \neq s,\end{cases} \tag{7}$$

$$\mathbf{U}_{ls}^{(0)T}\mathbf{T}_2\mathbf{U}_{ri}^{(0)} = -\lambda_i^{(0)}\delta_{is} = \begin{cases}-\lambda_i^{(0)}, & i = s\\ 0, & i \neq s.\end{cases} \tag{8}$$

When there is friction with the coefficient of friction $\mu = \varepsilon_\mu$ between the components of the system that is called the perturbation system, Equation (3), according to the matrix perturbation theory, there will be small changes both in eigenvalues and eigenvectors, so they can be expressed as the power series with respect to ε_μ which is the perturbation parameter; that is,

$$\lambda_i = \lambda_i^{(0)} + \varepsilon_\mu\lambda_i^{(1)} + \varepsilon_\mu^2\lambda_i^{(2)} + \cdots, \tag{9}$$

$$\mathbf{U}_{ri} = \mathbf{U}_{ri}^{(0)} + \varepsilon_\mu\mathbf{U}_{ri}^{(1)} + \varepsilon_\mu^2\mathbf{U}_{ri}^{(2)} + \cdots, \tag{10}$$

$$\mathbf{U}_{li} = \mathbf{U}_{li}^{(0)} + \varepsilon_\mu\mathbf{U}_{li}^{(1)} + \varepsilon_\mu^2\mathbf{U}_{li}^{(2)} + \cdots, \tag{11}$$

where $\lambda_i^{(n)}$, $\mathbf{U}_{ri}^{(n)}$, and $\mathbf{U}_{li}^{(n)}$ are nth order perturbation of λ_i, $\mathbf{U}_{ri}$, and $\mathbf{U}_{li}$, respectively.

Substituting (9)–(11) into perturbed system in (3), then

$$\begin{aligned}&\left[\left(\lambda_i^{(0)} + \varepsilon_\mu\lambda_i^{(1)} + \varepsilon_\mu^2\lambda_i^{(2)} + \cdots\right)\mathbf{T}_1\right.\\ &\quad\left.+\left(\mathbf{T}_2 + \varepsilon_\mu\mathbf{T}_{2,\varepsilon} + \varepsilon_\mu^2\mathbf{T}_{2,\varepsilon^2} + \cdots\right)\right]\cdot\left(\mathbf{U}_{ri}^{(0)} + \varepsilon_\mu\mathbf{U}_{ri}^{(1)}\right.\\ &\quad\left.+\varepsilon_\mu^2\mathbf{U}_{ri}^{(2)} + \cdots\right) = 0,\end{aligned} \tag{12a}$$

$$\begin{aligned}&\left[\left(\lambda_i^{(0)} + \varepsilon_\mu\lambda_i^{(1)} + \varepsilon_\mu^2\lambda_i^{(2)} + \cdots\right)\mathbf{T}_1\right.\\ &\quad\left.+\left(\mathbf{T}_2 + \varepsilon_\mu\mathbf{T}_{2,\varepsilon} + \varepsilon_\mu^2\mathbf{T}_{2,\varepsilon^2} + \cdots\right)\right]^T\cdot\left(\mathbf{U}_{li}^{(0)} + \varepsilon_\mu\mathbf{U}_{li}^{(1)}\right.\\ &\quad\left.+\varepsilon_\mu^2\mathbf{U}_{li}^{(2)} + \cdots\right) = 0.\end{aligned} \tag{12b}$$

Equating the terms of the same orders in (12a) yields

$$\varepsilon_\mu^0 : \left(\lambda_i^{(0)}\mathbf{T}_1 + \mathbf{T}_2\right)\mathbf{U}_{ri}^{(0)} = 0, \tag{13a}$$

$$\varepsilon_\mu^n : \sum_{k=0}^{n}\left(\lambda_i^{(k)}\mathbf{T}_1 + \mathbf{T}_{2,\varepsilon^k}\right)\mathbf{U}_{ri}^{(n-k)} = 0 \quad (n \geq 1). \tag{13b}$$

It can be seen that (13a) is exactly (5). Let the perturbed eigenvectors be expressed as a linear combination of the unperturbed eigenvectors as

$$\mathbf{U}_{ri}{}^{(n)} = \sum_{s=1}^{2N} C_{rsi}^{(n)}\mathbf{U}_{rs}^{(0)} \quad (i = 1, 2, \ldots, 2N). \tag{14}$$

Substituting (14) into (13b), premultiplying by $\mathbf{U}_{lp}^{(0)T}$ and using (7), (8) yields

$$\sum_{k=1}^{n}\left(\lambda_i^{(k)}C_{rpi}^{(n-k)} + \sum_{s=1}^{2N}C_{rsi}^{(n-k)}E_{ps}^{(k)}\right) + \left(\lambda_i^{(0)} - \lambda_p^{(0)}\right)C_{rpi}^{(n)} = 0, \tag{15}$$

where $C_{rpi}^{(0)} = \delta_{pi}$ and $E_{pi}^{(k)} = \mathbf{U}_{lp}^{(0)T}\mathbf{T}_{2,\varepsilon^k}\mathbf{U}_{ri}^{(0)}$ $(k \geq 1)$.

It can be obtained that

$$C_{rpi}^{(n)} = \frac{\sum_{k=1}^{n}\left(\lambda_i^{(k)}C_{rpi}^{(n-k)} + \sum_{s=1}^{2N}C_{rsi}^{(n-k)}E_{ps}^{(k)}\right)}{\lambda_p^{(0)} - \lambda_i^{(0)}}, \quad i \neq p, \tag{16}$$

$$\lambda_i^{(n)} = -\sum_{k=1}^{n-1}\left(\lambda_i^{(k)}C_{rii}^{(n-k)} + \sum_{s=1}^{2N}C_{rsi}^{(n-k)}E_{is}^{(k)}\right) - E_{ii}^{(n)}. \tag{17}$$

Similarly, equating the terms of the same orders in (12b) yields

$$\varepsilon_\mu^0 : \left(\lambda_i^{(0)}\mathbf{T}_1 + \mathbf{T}_2\right)^T\mathbf{U}_{li}^{(0)} = 0, \tag{18a}$$

$$\varepsilon_\mu^n : \sum_{k=0}^{n}\left(\lambda_i^{(k)}\mathbf{T}_1 + \mathbf{T}_{2,\varepsilon^k}\right)^T\mathbf{U}_{li}^{(n-k)} = 0 \quad (n \geq 1). \tag{18b}$$

It can be seen that (18a) is exactly (6). Let the perturbed eigenvectors be expressed as a linear combination of the unperturbed eigenvectors as

$$\mathbf{U}_{li}^{(n)} = \sum_{s=1}^{2N}C_{lsi}^{(n)}\mathbf{U}_{ls}^{(0)} \quad (i = 1, 2, \ldots, 2N). \tag{19}$$

Substituting (19) into (18b), premultiplying by $\mathbf{U}_{rp}^{(0)T}$ and using (7), (8) yields

$$\sum_{k=1}^{n}\left(\lambda_i^{(k)}C_{lpi}^{(n-k)} + \sum_{s=1}^{2N}C_{lsi}^{(n-k)}E_{ps}^{(k)}\right) + \left(\lambda_i^{(0)} - \lambda_p^{(0)}\right)C_{lpi}^{(n)} = 0, \tag{20}$$

where $C_{lpi}^{(0)} = \delta_{pi}$.

It can be obtained that

$$C_{lpi}^{(n)} = \frac{\sum_{k=1}^{n}\left(\lambda_i^{(k)}C_{lpi}^{(n-k)} + \sum_{s=1}^{2N}C_{lsi}^{(n-k)}E_{ps}^{(k)}\right)}{\lambda_p^{(0)} - \lambda_i^{(0)}}, \quad i \neq p, \tag{21}$$

$$\lambda_i^{(n)} = -\sum_{k=1}^{n-1}\left(\lambda_i^{(k)}C_{lii}^{(n-k)} + \sum_{s=1}^{2N}C_{lsi}^{(n-k)}E_{is}^{(k)}\right) - E_{ii}^{(n)}. \tag{22}$$

$C_{rii}^{(n)}$ and $C_{lii}^{(n)}$, $(i = 1, 2, \ldots, n)$, can be obtained using the normalization condition of the eigenvectors; the right eigenvectors $\mathbf{U}_{ri}$ and the left eigenvectors $\mathbf{U}_{li}$ should satisfy the condition

$$\mathbf{U}_{li}^T\mathbf{T}_1\mathbf{U}_{ri} = 1. \tag{23}$$

Substituting (10) and (11) into (23) yields

$$\left(\mathbf{U}_{li}^{(0)} + \varepsilon_\mu\mathbf{U}_{li}^{(1)} + \varepsilon_\mu^2\mathbf{U}_{li}^{(2)} + \cdots\right)^T \cdot \mathbf{T}_1\left(\mathbf{U}_{ri}^{(0)} + \varepsilon_\mu\mathbf{U}_{ri}^{(1)} + \varepsilon_\mu^2\mathbf{U}_{ri}^{(2)} + \cdots\right) = 1. \tag{24}$$

Equating the terms of the same orders in (24) yields

$$\varepsilon_\mu^0 : \mathbf{U}_{li}^{(0)T}\mathbf{T}_1\mathbf{U}_{ri}^{(0)} = 1, \tag{25a}$$

$$\varepsilon_\mu^n : \sum_{k=0}^{n}\mathbf{U}_{li}^{(k)T}\mathbf{T}_1\mathbf{U}_{ri}^{(n-k)} = 0 \quad (n \geq 1). \tag{25b}$$

It can be seen that (25a) is exactly (7). Substituting (14) and (19) into (25b) using (7), (8) yields

$$C_{rii}^{(n)} + C_{lii}^{(n)} + \sum_{k=1}^{n-1}\left[\sum_{s=1}^{2N}C_{lsi}^{(k)}C_{rsi}^{(n-k)}\right] = 0. \tag{26}$$

It is obvious that $\lambda_i^{(n)}$ in (17) and (22) should be the same, so that

$$C_{rii}^{(n)} = C_{lii}^{(n)} \tag{27}$$

so it can be obtained that

$$C_{rii}^{(n)} = C_{lii}^{(n)} = -\frac{1}{2}\sum_{k=1}^{n-1}\left[\sum_{s=1}^{2N}C_{lsi}^{(k)}C_{rsi}^{(n-k)}\right]. \tag{28}$$

It is obvious that $\lambda_i^{(n)}$ $(i = 1, 2, \ldots, 2N, n = 1, 2, \ldots)$ can be obtained using the above equations.

2.2. Use of Huang's Method. The above-mentioned method will be invalid when the mode coupling takes place. So Huang's method is used here to obtain the influential eigenfrequencies. The characteristic equation for the two coupling eigenfrequencies is a 2nd order polynomial in λ that can be factored into the following form:

$$f(\lambda) = \lambda^2 + b(\mu)\lambda + c(\mu) = 0, \tag{29}$$

where $b(\mu) = \sum_{p=1}^{M} b_p \mu^{p-1}$, $c(\mu) = \sum_{p=1}^{M} c_p \mu^{p-1}$, and b_p, c_p are sets of M (the largest perturbation order $\geq M$) yet-to-be-determined coefficients.

Assuming that λ_s and λ_t are the two coupling eigenfrequencies for perturbed system, the coefficients b_p, c_p can be determined by matching known values of $\lambda_s^{(0)}$, $\lambda_t^{(0)}$, and their derivatives $\lambda_s^{(n)}$, $\lambda_t^{(n)}$ $(n = 1, 2, \ldots)$ as

$$f(\lambda_s)|_{\mu=0} = \lambda_s^{(0)2} + b_1 \lambda_s^{(0)} + c_1 = 0, \tag{30a}$$

$$\left.\frac{d^i f(\lambda_s)}{d\mu^i}\right|_{\mu=0} = \sum_{p=0}^{i} \frac{i!}{p!} b_{i+1-p} \lambda_s^{(p)} + i! c_{i+1} + \sum_{p=0}^{i} \frac{i!}{(i-p)!\,p!} \lambda_s^{(p)} \lambda_s^{(i-p)} = 0 \quad (i = 1, 2, \ldots, M), \tag{30b}$$

where $\lambda_s^{(k)} = (d^k \lambda_s / d\mu^k)|_{\mu=0}$ and the same for λ_t.

The coefficients b_p and c_p can be solved explicitly from (30a) and (30b) to produce for $i = 1, 2, \ldots, M$

$$b_i = -\left(\lambda_s^{(i-1)} + \lambda_t^{(i-1)}\right), \tag{31a}$$

$$c_i = \sum_{p=0}^{i-1} \lambda_s^{(p)} \lambda_t^{(i-1-p)}. \tag{31b}$$

Using (31a) and (31b), the roots of (29) define the two eigenvalues λ_s and λ_t, which is called original perturbation in this paper.

2.3. Judge the Influential Eigenfrequencies. If only the eigenfrequencies belonging to the set Γ are taken into account when calculating λ_s and λ_t using the above-mentioned method, then when calculating $C_{rpi}^{(n)}$ in (16), $C_{lpi}^{(n)}$ in (21), and $\lambda_i^{(n)}$ in (17), $\sum_{s=1}^{2N}$ should be replaced by $\sum_{s\in\Gamma}$. In this way, the corresponding λ_s^* and λ_t^* that rule out the eigenfrequencies not belonging to the set Γ can also be obtained, which is called reduced-order perturbation in this paper. If ruling out the eigenfrequencies not belonging to the set Γ, λ_s^* and λ_t^* change little (in the permissible range) compared with λ_s and λ_t; then, the set Γ is called the influential set Γ^* in this paper. Note that this method will save much time compared with the complex eigenvalue analysis at every given friction coefficient.

3. The Reduced-Order Model

Substituting (4) into (2), the original model changes to

$$\mathbf{T}_1 \dot{\mathbf{z}} + \left(\mathbf{T}_2 + \varepsilon_\mu \mathbf{T}_{2,\varepsilon} + \varepsilon_\mu^2 \mathbf{T}_{2,\varepsilon^2} + \cdots\right) \mathbf{z} = \mathbf{0}. \tag{32}$$

The coordinates $\mathbf{z}$ are transformed to a new set of coordinates $\boldsymbol{\eta}$ such that

$$\mathbf{z} = \mathbf{U}_r^{(0)} \boldsymbol{\eta}, \tag{33}$$

where $\mathbf{U}_r^{(0)} = (\mathbf{U}_{r1}^{(0)}, \mathbf{U}_{r2}^{(0)}, \ldots, \mathbf{U}_{r,2N}^{(0)})$.

Premultiplying by $\mathbf{U}_l^{(0)T}$ gives

$$\dot{\boldsymbol{\eta}} + \left(-\operatorname{diag}\left(\lambda_1^{(0)}, \lambda_2^{(0)}, \ldots, \lambda_{2N}^{(0)}\right) + \varepsilon_\mu \begin{bmatrix} E_{11}^{(1)} & \cdots & E_{1,2N}^{(1)} \\ \vdots & & \\ E_{2N,1}^{(1)} & \cdots & E_{2N,2N}^{(1)} \end{bmatrix} + \varepsilon_\mu^2 \begin{bmatrix} E_{11}^{(2)} & \cdots & E_{1,2N}^{(2)} \\ \vdots & & \\ E_{2N,1}^{(2)} & \cdots & E_{2N,2N}^{(2)} \end{bmatrix} + \cdots \right) \boldsymbol{\eta} = \mathbf{0}, \tag{34}$$

where $\mathbf{U}_l^{(0)} = (\mathbf{U}_{l1}^{(0)}, \mathbf{U}_{l2}^{(0)}, \ldots, \mathbf{U}_{l,2N}^{(0)})$.

Then, the reduced-order model is obtained as

$$\dot{\boldsymbol{\eta}} + \left(-\begin{bmatrix} \lambda_i^{(0)} & & \\ & \lambda_j^{(0)} & \\ & & \ddots \end{bmatrix} + \varepsilon_\mu \begin{bmatrix} E_{ii}^{(1)} & E_{ji}^{(1)} & \\ E_{ij}^{(1)} & E_{jj}^{(1)} & \\ & & \ddots \end{bmatrix} + \varepsilon_\mu^2 \begin{bmatrix} E_{ii}^{(2)} & E_{ji}^{(2)} & \\ E_{ij}^{(2)} & E_{jj}^{(2)} & \\ & & \ddots \end{bmatrix} + \cdots \right) \boldsymbol{\eta} = \mathbf{0}, \tag{35}$$

where $i, j, \ldots \in \Gamma^*$.

Equation (35) can also be expressed as

$$\dot{\boldsymbol{\eta}} + \begin{bmatrix} \mathbf{U}_{li}^{(0)T} \mathbf{T}_2' \mathbf{U}_{ri}^{(0)} & \mathbf{U}_{lj}^{(0)T} \mathbf{T}_2' \mathbf{U}_{ri}^{(0)} & \\ \mathbf{U}_{li}^{(0)T} \mathbf{T}_2' \mathbf{U}_{rj}^{(0)} & \mathbf{U}_{lj}^{(0)T} \mathbf{T}_2' \mathbf{U}_{rj}^{(0)} & \\ & & \ddots \end{bmatrix} \boldsymbol{\eta} = \mathbf{0}, \tag{36}$$

where $i, j, \ldots \in \Gamma^*$.

Note that $\lambda_i^{(n)*}$ (the nth order perturbation of λ_i corresponding to the reduced-order model) can be obtained just if $\sum_{s=1}^{2N}$ is replaced by $\sum_{s\in\Gamma^*}$ when calculating $C_{rpi}^{(n)}$ in (16), $C_{lpi}^{(n)}$ in (21), and $\lambda_i^{(n)}$ in (17). After using the method mentioned in Section 2.2, the solutions are just λ_s^* and λ_t^*. In conclusion, when λ_s^* and λ_t^* are close enough to λ_s and λ_t, respectively, then the two coupling eigenfrequencies solved in the reduced-order model will get close enough to those solved in the original model. So this reduced-order model is useful when predicting the onset of squeal and the squeal frequency.

It is assumed that there are no repeated eigenvalues for the unperturbed system; that is, $\lambda_i^{(0)} \neq \lambda_s^{(0)}$ $(i \neq s)$, which is typically true for brake system without friction. If there are repeated eigenvalues for the unperturbed system, other methods such as matrix perturbation theory for multiple eigenvalues [11] can be used to calculate $\lambda_i^{(n)}$ $(i = 1, 2, \ldots, 2N$, $n = 1, 2, \ldots)$. Also note that the same approach can be used for system with one parameter other than the coefficient of friction and also for system with more than one parameter.

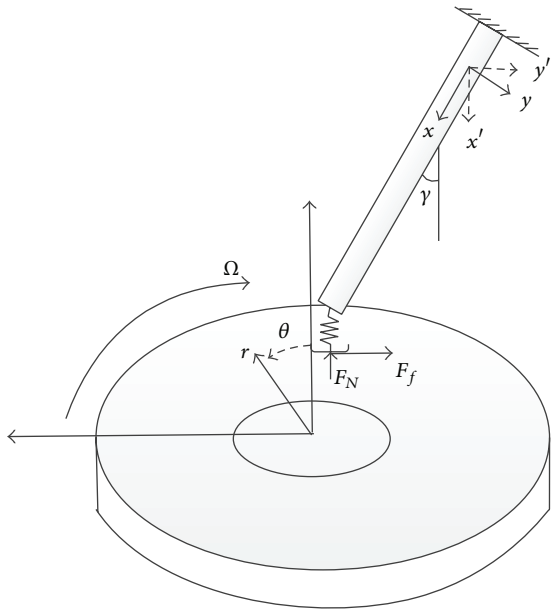

Figure 1: The pin-on-disc system.

4. Example of Application of the Reduced-Order Model

4.1. Flexible Pin-on-Disc System

4.1.1. Pin-on-Disc Transient Model. The pin-on-disc system used in the present study consists of two components: (i) a flexible disc and (ii) a flexible pin, as shown in Figure 1. The disc is assumed to be clamped at the inner rim and free at the outer rim. The pin has a uniform round cross-sectional area and is assumed to be fully clamped at one end and in contact with the disc at the other end. It is assumed that the pin can vibrate in two principal directions: the axis direction, x, and the transverse direction, y, whereas the disc can vibrate only in the out-of-plane direction, w. One end of the pin is contact with the disc, which rotates at the constant speed of Ω, with a contact stiffness of K. The pin inclines with an angle of γ along the direction of rotation of the disc. Since disc brake squeal tends to appear at low speeds [12] when centripetal and gyroscopic effects may be omitted. The effect of friction follower force is neglected on the basis that contact stiffness term is much larger than preload term in the stiffness matrix [5, 13].

As is depicted in Figure 1, the disc is rotating at the constant speed of Ω, there is a preload F_L between the pin and disc. There are three coordinate systems in the model, which are the absolute coordinate systems $(\tilde{r}, \tilde{\theta})$, the coordinate systems (r, θ) fixed on the disc, and the coordinate systems (x, y) fixed on the pin, respectively. Assume that at the beginning, the coordinate of the free end of the pin in the coordinate systems (r, θ) is $(r_0, 0)$. At the moment t, the rotational angle of the free end of the pin relative to the axis of the disc is $\psi(t)$, and the rotational angle of the free end of the pin relative to that of the disc is $\varphi(t)$, so $\psi = \Omega t - \varphi$. Rotational effects and the effect of friction follower force are neglected and the equation of motion of the disc in the coordinate systems (r, θ) is

$$\begin{aligned} \rho_p h \frac{\partial^2 w}{\partial t^2} + D\nabla^4 w + D^* \nabla^4 \frac{\partial w(r,\theta,t)}{\partial t} \\ = -\frac{1}{r}\Big[\delta(r-r_0)\,\delta(\theta-\varphi)\,F_N \\ - \frac{\partial}{r\partial\theta}\left(M(t)\,\delta(\theta-\varphi)\right)\delta(r-r_0)\Big], \end{aligned} \tag{37}$$

where $M(t) = \mu\,\mathrm{sign}(\dot{\varphi}) F_N (h/2)$ is the moment acting on the disc.

The transverse vibration of the pin in the coordinate systems (x, y) can be written as

$$\begin{aligned} E_p I \frac{\partial^4 u^t}{\partial x^4} + \rho_p S \frac{\partial^2 u^t}{\partial t^2} + c_t I \frac{\partial^5 u^t(x,t)}{\partial x^4 \partial t} \\ = \delta(x-l)\,F_N\left[-\sin\gamma + \mu\,\mathrm{sign}(\dot{\varphi})\cos\gamma\right]. \end{aligned} \tag{38}$$

Similarly, the axial vibration of the pin in the coordinate system (x, y) can be written as

$$\begin{aligned} \rho_p S \frac{\partial^2 u^a}{\partial t^2} - E_p S \frac{\partial^2 u^a}{\partial x^2} - c_a S \frac{\partial^3 u^a}{\partial x^2 \partial t} \\ = \delta(x-l)\,F_N\left(\cos\gamma + \mu\,\mathrm{sign}(\dot{\varphi})\sin\gamma\right). \end{aligned} \tag{39}$$

Assuming that the free end of the pin is in constant contact with the disc with a contact stiffness of K, the transverse displacement of the disc at the contact point between them can be derived as

$$d_K(t) = w(r_0, \varphi(t), t). \tag{40}$$

To transform the deflection of the pin in the coordinate system (x, y) to (x', y') (shown in Figure 1), the transformation matrix $D^{x,y\to x',y'} = \begin{bmatrix} \cos\gamma & \sin\gamma \\ -\sin\gamma & \cos\gamma \end{bmatrix}$ can be derived. The deflection of the pin in the coordinate system (x', y') is $D^{x,y\to x',y'} \begin{bmatrix} -u^a(l,t) \\ u^t(l,t) \end{bmatrix} = \begin{bmatrix} -u^a(l,t)\cos\gamma + u^t(l,t)\sin\gamma \\ u^a(l,t)\sin\gamma + u^t(l,t)\cos\gamma \end{bmatrix}$, so the normal force acting on the pin can be obtained as

$$F_N = K\left(-u^a(l,t)\cos\gamma + u^t(l,t)\sin\gamma + d_K(t)\right) + F_L. \tag{41}$$

The transverse vibration of the disc can be expressed by the summation of its natural modes and modal coordinates as

$$w(r,\theta,t) = \sum_{k=0}^{\infty}\sum_{l=-\infty}^{\infty} \Phi_{kl}(r,\theta)\,q_{kl}(t), \tag{42}$$

where $\Phi_{kl}(r,\theta) = R_{kl}(r)\exp(jl\theta)$ $(k = 0, 1, 2, \ldots;\ l = 0, \pm 1, \pm 2, \ldots)$ which satisfy the orthonormality conditions,

$$\begin{aligned} \rho_p h \iint_{CS} \Phi_{kl}\overline{\Phi}_{rs}\, r\,\mathrm{d}r\,\mathrm{d}\theta = \delta_{kr}\delta_{ls}, \\ D\iint_{CS} \nabla^4 \Phi_{kl}\overline{\Phi}_{rs}\, r\,\mathrm{d}r\,\mathrm{d}\theta = \omega_{kl}^2 \delta_{kr}\delta_{ls}, \end{aligned} \tag{43}$$

where $\iint_{CS} = \int_0^{2\pi}\int_a^b$ and the bar over a symbol denotes the complex conjugation.

(Note that the mode shapes of the disc are in the form of nodal circles and nodal diameters denoted, resp., by the subscripts k and l.).

Similarly, the transverse vibration of the pin can be expressed by the summation of its natural modes and modal coordinates as

$$u^t(x,t) = \sum_{i=1}^{\infty}\varphi_i^t(x)\,p_i^t(t) \tag{44}$$

which satisfy the orthonormality conditions:

$$\begin{aligned}\rho_p S\int_0^l \varphi_i^t(x)\,\varphi_s^t(x)\,\mathrm{d}x &= \delta_{is},\\ E_p I\int_0^l \frac{\mathrm{d}^4\varphi_i^t(x)}{\mathrm{d}x^4}\varphi_s^t(x)\,\mathrm{d}x &= \omega_i^{t2}\delta_{is}.\end{aligned} \tag{45}$$

The axial vibration of the pin can be expressed by the summation of its natural modes and modal coordinates as

$$u^a(x,t) = \sum_{i=1}^{\infty}\varphi_i^a(x)\,p_i^a(t) \tag{46}$$

which satisfy the orthonormality conditions:

$$\begin{aligned}\rho_p S\int_0^l \varphi_i^a(x)\,\varphi_s^a(x)\,\mathrm{d}x &= \delta_{is},\\ -E_p S\int_0^l \frac{\mathrm{d}^2\varphi_i^a(x)}{\mathrm{d}x^2}\varphi_s^a(x)\,\mathrm{d}x &= \omega_i^{a2}\delta_{is}.\end{aligned} \tag{47}$$

With regard to the disc, substituting (42), (44), and (46) into (37), multiplying (37) with $\overline{\Phi}_{rs}$, and then integrating with the help of (43) yields

$$\begin{aligned}&q_{rs}''(t) + \frac{D^*}{D}\omega_{rs}^2 q_{rs}'(t) + \omega_{rs}^2 q_{rs}(t)\\ &\quad= -\Bigg[K\Bigg(-\sum_{i=1}^{\infty}\varphi_i^a(l)\,p_i^a(t)\cos\gamma\\ &\qquad+\sum_{i=1}^{\infty}\varphi_i^t(l)\,p_i^t(t)\sin\gamma\\ &\qquad+\sum_{k=0}^{\infty}\sum_{l=-\infty}^{\infty}\Phi_{kl}(r_0,\varphi)\,q_{kl}(t)\Bigg)+F_L\Bigg]\overline{\Phi}_{rs}(r_0,\varphi)\\ &\qquad+\frac{j\mu sh}{2r_0}\operatorname{sign}(\dot\varphi)\,R_{rs}(r_0)\exp(-js\varphi)\\ &\qquad\cdot\Bigg[K\Bigg(-\sum_{i=1}^{\infty}\varphi_i^a(l)\,p_i^a(t)\cos\gamma+\sum_{i=1}^{\infty}\varphi_i^t(l)\,p_i^t(t)\sin\gamma\\ &\qquad+\sum_{k=0}^{\infty}\sum_{l=-\infty}^{\infty}\Phi_{kl}(r_0,\varphi)\,q_{kl}(t)\Bigg)+F_L\Bigg].\end{aligned} \tag{48}$$

Similarly, with regard to the transverse vibration of the pin, substituting (42), (44), and (46) into (38), multiplying (38) with $\varphi_s^t(x)$, and then integrating with the help of (43) yields

$$\begin{aligned}&p_s^{t''}(t) + \frac{c_t}{E_p}\omega_s^{t2}p_s^{t'}(t) + \omega_s^{t2}p_s^t(t)\\ &\quad= \Bigg[K\Bigg(-\sum_{i=1}^{\infty}\varphi_i^a(l)\,p_i^a(t)\cos\gamma\\ &\qquad+\sum_{i=1}^{\infty}\varphi_i^t(l)\,p_i^t(t)\sin\gamma\\ &\qquad+\sum_{k=0}^{\infty}\sum_{l=-\infty}^{\infty}\Phi_{kl}(r_0,\varphi)\,q_{kl}(t)\Bigg)+F_L\Bigg][-\sin\gamma+\mu\\ &\qquad\cdot\operatorname{sign}(\dot\varphi)\cos\gamma]\,\varphi_s^t(l).\end{aligned} \tag{49}$$

Similarly, with regard to the axial vibration of the pin, substituting (42), (44), and (46) into (39), multiplying (39) with $\varphi_s^a(x)$, and then integrating with the help of (43) yields

$$\begin{aligned}&p_s^{a''}(t) + \frac{c_a}{E_p}\omega_s^{a2}p_s^{a'}(t) + \omega_s^{a2}p_s^a(t)\\ &\quad= \Bigg[K\Bigg(-\sum_{i=1}^{\infty}\varphi_i^a(l)\,p_i^a(t)\cos\gamma+\sum_{i=1}^{\infty}\varphi_i^t(l)\,p_i^t(t)\sin\gamma\\ &\qquad+\sum_{k=0}^{\infty}\sum_{l=-\infty}^{\infty}\Phi_{kl}(r_0,\varphi)\,q_{kl}(t)\Bigg)+F_L\Bigg](\cos\gamma+\mu\\ &\qquad\cdot\operatorname{sign}(\dot\varphi)\sin\gamma)\,\varphi_s^a(l).\end{aligned} \tag{50}$$

Considering that $\psi = \Omega t - \varphi = (u^a(l,t)\sin\gamma + u^t(l,t)\cos\gamma)/r_0$ is marginal compared with Ωt, so for the sake of simplification, ψ is neglected in the model so that $\varphi = \Omega t$.

To make use of the method of state space, new modal coordinates are introduced as

$$\begin{aligned}&x_{kl}(t) = q_{kl}(t)\exp(jl\varphi)\\ &\qquad(k = 0,1,2,\ldots;\, l = 0,\pm1,\pm2,\ldots),\\ &p_i^t(t)\quad(i = 1,2,\ldots),\\ &p_i^a(t)\quad(i = 1,2,\ldots).\end{aligned} \tag{51}$$

Equations (48), (49), and (50) then become

$$\begin{aligned}
&x_{rs}''(t) - 2js\varphi' x_{rs}'(t) - s^2\varphi'^2 x_{rs}(t) + \frac{D^*}{D}\omega_{rs}^2\left(x_{rs}'(t)\right.\\
&\quad\left. - js\varphi' x_{rs}(t)\right) + \omega_{rs}^2 x_{rs}(t)\\
&\quad = -\left[K\left(-\sum_{i=1}^{\infty}\varphi_i^a(l)\,p_i^a(t)\cos\gamma\right.\right.\\
&\quad\left.\left. + \sum_{i=1}^{\infty}\varphi_i^t(l)\,p_i^t(t)\sin\gamma + \sum_{k=0}^{\infty}\sum_{l=-\infty}^{\infty}R_{kl}(r_0)\,x_{kl}(t)\right)\right.\\
&\quad\left. + F_L\right]R_{rs}(r_0) + \frac{j\mu sh}{2r_0}\operatorname{sign}(\dot\varphi)\,R_{rs}(r_0)\\
&\quad\cdot\left[K\left(-\sum_{i=1}^{\infty}\varphi_i^a(l)\,p_i^a(t)\cos\gamma + \sum_{i=1}^{\infty}\varphi_i^t(l)\,p_i^t(t)\sin\gamma\right.\right.\\
&\quad\left.\left. + \sum_{k=0}^{\infty}\sum_{l=-\infty}^{\infty}R_{kl}(r_0)\,x_{kl}(t)\right) + F_L\right],\\
&p_s^{t''}(t) + \frac{c_t}{E}\omega_s^{t2}p_s^{t'}(t) + \omega_s^{t2}p_s^t(t)\\
&\quad = \left[K\left(-\sum_{i=1}^{\infty}\varphi_i^a(l)\,p_i^a(t)\cos\gamma + \sum_{i=1}^{\infty}\varphi_i^t(l)\,p_i^t(t)\sin\gamma\right.\right.\\
&\quad\left.\left. + \sum_{k=0}^{\infty}\sum_{l=-\infty}^{\infty}R_{kl}(r_0)\,x_{kl}(t)\right) + F_L\right]\left[-\sin\gamma + \mu\right.\\
&\quad\left.\cdot\operatorname{sign}(\dot\varphi)\cos\gamma\right]\varphi_s^t(l),\\
&p_s^{a''}(t) + \frac{c_a}{E}\omega_s^{a2}p_s^{a'}(t) + \omega_s^{a2}p_s^a(t)\\
&\quad = \left[K\left(-\sum_{i=1}^{\infty}\varphi_i^a(l)\,p_i^a(t)\cos\gamma + \sum_{i=1}^{\infty}\varphi_i^t(l)\,p_i^t(t)\sin\gamma\right.\right.\\
&\quad\left.\left. + \sum_{k=0}^{\infty}\sum_{l=-\infty}^{\infty}R_{kl}(r_0)\,x_{kl}(t)\right) + F_L\right]\left(\cos\gamma + \mu\right.\\
&\quad\left.\cdot\operatorname{sign}(\dot\varphi)\sin\gamma\right)\varphi_s^a(l).
\end{aligned} \tag{52}$$

4.1.2. Friction Model. The velocity-dependent friction model used in this study is reasonably described with well-known exponential formulation. The coefficient of dynamic friction is introduced as [14]. Consider

$$\mu = \mu(V_{rel}) = \mu_d\left[1 + \left(\frac{\mu_s}{\mu_d} - 1\right)e^{-\beta|V_{rel}|}\right], \tag{53}$$

$$\begin{aligned}
V_{rel} &= r_0\dot\varphi = r_0\Omega - \frac{\partial u^a(l,t)}{\partial t}\sin\gamma - \frac{\partial u^t(l,t)}{\partial t}\cos\gamma\\
&= r_0\Omega - \mathbf{R}_C\dot{\mathbf{y}},
\end{aligned} \tag{54}$$

where μ_s governs the larger relative velocity behavior, μ_d denotes the static friction coefficient, and β controls the gradient of μ relative to V_{rel}. $\mathbf{R}_C$ and $\mathbf{y}$ are provided in the Appendix.

4.1.3. Linearization of the Model. The onset of squeal is widely believed to be due to an unstable behavior occurring in linear conditions during the braking phase, linearization of the nonlinear system is conducted around the static equilibrium point for various system parameters, and only small perturbation around the static equilibrium point is considered. The friction coefficient in (53) is linearized via Taylor series as follows:

$$\mu = \mu_0 - S_1\mathbf{R}_C\dot{\mathbf{y}} + o\left(\left(\mathbf{R}_C\dot{\mathbf{y}}\right)^2\right), \tag{55}$$

where $\mu_0 = \mu(r_0\Omega)$ is the friction coefficient at the speed of the contact point between the pin and disc. $S_1 = (\partial\mu/\partial V_{rel})|_{V_{rel}=r_0\Omega}$ is the slope of the friction coefficient at the same point.

By defining $(D^*/D)\omega_{rs}^2 = 2\xi_{rs}\omega_{rs}$, $(c_t/E_p)\omega_s^{t2} = 2\xi_s^t\omega_s^t$, and $(c_a/E_p)\omega_s^{a2} = 2\xi_s^a\omega_s^a$, the static equilibrium point can be easily determined by forcing all time derivative terms to zero in (25a), (25b), (26), (27), (30a), and (30b) as follows:

$$\begin{aligned}
&\left(-\Omega^2\mathbf{D} + j\Omega\mathbf{C}\mathbf{C}_s + \left[\omega^2\right] + K\mathbf{A} + \mu_0 K\operatorname{sign}(\dot\varphi)\,\mathbf{B}\right)\mathbf{y}^*\\
&\quad = -F_L\mathbf{R}_A^T + \mu_0\operatorname{sign}(\dot\varphi)\,F_L\left(\mathbf{R}_C^T - \frac{jh}{2r_0}\mathbf{C}^T\mathbf{R}_A^T\right),
\end{aligned} \tag{56}$$

where $\mathbf{D}$, $\mathbf{C}$, $\mathbf{C}_s$, $[\omega^2]$, $\mathbf{A}$, $\mathbf{B}$, and $\mathbf{R}_A$ are also provided in the Appendix.

Assuming small perturbation around the static equilibrium point, that is, $\mathbf{y} = \mathbf{Y} + \mathbf{y}^*$, and neglecting $\dot{\mathbf{Y}}\mathbf{Y}$, leads to the following linearized system:

$$\begin{aligned}
&\ddot{\mathbf{Y}} + j2\Omega\mathbf{C}\dot{\mathbf{Y}} - \Omega^2\mathbf{D}\mathbf{Y} + \mathbf{C}_s\dot{\mathbf{Y}} + j\Omega\mathbf{C}\mathbf{C}_s\mathbf{Y} + \left[\omega^2\right]\mathbf{Y}\\
&\quad + K\mathbf{A}\mathbf{Y} + \mu_0 K\operatorname{sign}(\dot\varphi)\,\mathbf{B}\mathbf{Y}\\
&\quad - S_1 K\operatorname{sign}(\dot\varphi)\,\mathbf{B}\mathbf{y}^*\mathbf{R}_C\dot{\mathbf{Y}}\\
&\quad + S_1\operatorname{sign}(\dot\varphi)\,F_L\left(\mathbf{R}_C^T - \frac{jh}{2r_0}\mathbf{C}^T\mathbf{R}_A^T\right)\mathbf{R}_C\dot{\mathbf{Y}} = 0,
\end{aligned} \tag{57}$$

where $\mathbf{C}$ is the damping matrix, $[\omega^2]$ is the natural frequency matrix of the disc and pin, $\mathbf{A} = \mathbf{A}^T$ is the contact stiffness matrix resulting from the contact between the disc and pin, $\mathbf{B} \neq \mathbf{B}^T$ is the complex nonsymmetric nonconservative work matrix produced by friction.

4.2. Application to This System. Obviously, it can be obtained from (32) that

$$\mathbf{K}_1' + \mu_0 K\operatorname{sign}(\dot\varphi)\,\mathbf{B} = \mathbf{K}_1, \tag{58}$$

where $\mathbf{K}_1$ is complex asymmetric because of the effect of the frictional force and the rotation of the disc, and $\mathbf{K}_1' = -\Omega^2\mathbf{D} + j\Omega\mathbf{C}\mathbf{C}_s + [\omega^2] + K\mathbf{A}$:

$$\begin{aligned}
&j2\Omega\mathbf{C} + \mathbf{C}_s - S_1 K\operatorname{sign}(\dot\varphi)\,\mathbf{B}\mathbf{y}^*\mathbf{R}_C\\
&\quad + S_1\operatorname{sign}(\dot\varphi)\,F_L\left(\mathbf{R}_C^T - \frac{jh}{2r_0}\mathbf{C}^T\mathbf{R}_A^T\right)\mathbf{R}_C = \mathbf{C}_1,
\end{aligned} \tag{59}$$

where $\mathbf{C}_1$ is complex asymmetric because of the rotation of the disc and nonlinearity.

Choose the perturbation parameter as $\varepsilon_\mu = \mu_0$. In (56), $\mathbf{y}^*$ can be expressed as the power series expansions with respect to ε_μ:

$$\mathbf{y}^* = -F_L \mathbf{K}_1'^{-1} \mathbf{R}_A^T + \sum_{k=1}^{n} \left(\varepsilon_\mu \operatorname{sign}(\dot{\varphi})\right)^k \mathbf{R}_k + \cdots, \tag{60}$$

where $\mathbf{R}_k = F_L[-(-K\mathbf{K}_1'^{-1}\mathbf{B})^k \mathbf{K}_1'^{-1}\mathbf{R}_A^T + (-K\mathbf{K}_1'^{-1}\mathbf{B})^{k-1}\mathbf{K}_1'^{-1}(\mathbf{R}_C^T - (jh/2r_0)\mathbf{C}^T\mathbf{R}_A^T)]$ $(k \geq 1)$.

Then, consider the following power series expansions for $\mathbf{T}_2'$ with respect to ε_μ:

$$\mathbf{T}_2' = \mathbf{T}_2 + \sum_{k=1}^{n} \varepsilon_\mu^k \mathbf{T}_{2,\varepsilon^k} + \cdots, \tag{61}$$

where

$$\begin{aligned}
\mathbf{T}_2 &= \begin{bmatrix} \mathbf{O} & -\mathbf{I} \\ \mathbf{K}_1' & \mathbf{C}_1' \end{bmatrix}, \\
\mathbf{T}_{2,\varepsilon} &= \begin{bmatrix} \mathbf{O} & \mathbf{O} \\ K\mathbf{B} & -S_1 K \mathbf{B}\mathbf{R}_1\mathbf{R}_C \end{bmatrix}, \\
\mathbf{T}_{2,\varepsilon^k} &= \begin{bmatrix} \mathbf{O} & \mathbf{O} \\ \mathbf{O} & -S_1 K \mathbf{B}\mathbf{R}_k\mathbf{R}_C \end{bmatrix} \quad (k \geq 2), \\
\mathbf{C}_1' &= j2\Omega\mathbf{C} + \mathbf{C}_s \\
&\quad - S_1 K \operatorname{sign}(\dot{\varphi})\, \mathbf{B}\left(-F_L \mathbf{K}_1'^{-1}\mathbf{R}_A^T\right)\mathbf{R}_C \\
&\quad + S_1 \operatorname{sign}(\dot{\varphi})\, F_L \left(\mathbf{R}_C^T - \frac{jh}{2r_0}\mathbf{C}^T\mathbf{R}_A^T\right)\mathbf{R}_C.
\end{aligned} \tag{62}$$

$\operatorname{sign}(\dot{\varphi})$ reduces to 1 since for small oscillations around the equilibrium point; the free end of the pin has such a low velocity that it does not reach the rotation speed of the disc.

In this section, the physical parameters used for the disc and pin are given in Tables 1 and 2, respectively. The problem of squeal is considered in a frequency range of 1–12 kHz so that only the first 13 modes of the disc, the 2nd and 3rd bending mode of the pin, and the first axial mode of the pin are used, so $N = 16$.

The eigenvalues $\lambda_i^{(0)}$ for the unperturbed system can be sorted with the ascending order of the imaginary part such as $\lambda_1^{(0)}, \lambda_2^{(0)}, \ldots, \lambda_{2N}^{(0)}$. Firstly, the parameters are assumed to be $K = 8 \times 10^8$ N/m, $r_0 = 0.09$ m, $\gamma = 5^\circ$, $\Omega = 20$ rad/s, $S_1 = 0$, and $D^* = c_t = c_a = 0$ so that a plot of predicted frequency (i.e., imaginary parts of eigenvalues) as a function of μ_0 in a frequency range of 1–12 kHz can be derived, as is shown in Figures 2(a) and 2(b).

Figure 2(a) shows that, in the frequency range of 1–6 kHz, frequency 23 coalesces with frequency 24 when μ_0 reaches 0.25, and there might be many frequencies having effect on this pair of coupling frequencies. Figure 2(b) shows that in the frequency range of 6–11 kHz, frequency 29 coalesces with frequency 30 when μ_0 reaches 0.09; however, there might be few frequencies having influence on this pair of coupling frequencies.

Table 1: Physical parameters used for the disc.

Component	a/mm	b/mm	h/mm	E_d/MPa	ν_d	ρ_d/kg·m^3
Disc	50	120	15	122000	0.23	7.19×10^3

Table 2: Physical parameters used for the pin.

Component	l/mm	d/mm	E_p/MPa	ν_p	ρ_p/kg·m^3
Pin	180	22	85000	0.32	2.88×10^3

Using the above-mentioned method, the influential set can be determined as $\Gamma^* = \{21, 22, 23, 24, 25, 30, 32\}$ corresponding to frequencies 23 and 24, and the effect of the reduced-order model is shown in Figure 3(a) that when the reduced-order perturbation gets close to the original perturbation, the error of reduced-order model with respect to the exact is always less than 20 Hz, which is a satisfactory result. Note that the frequencies solved from the original model are called "exact" solutions here. The same is for frequencies 29 and 30 when choosing $\Gamma^* = \{29, 30, 32\}$; as is shown in Figure 3(b), there is hardly any error between the result of reduced-order model and the exact.

A more complicated example is shown in Figures 4(a) and 4(b), when taking the damping $D^* = c_t = c_a = 0.05\,\mathrm{N \cdot s/m}$ and nonlinearity $S_1 = -0.1$ s/m into account. The influential set can also be determined as $\Gamma^* = \{21, 22, 23, 24, 25, 30, 32\}$ corresponding to frequencies 23 and 24, and the effect of the reduced-order model is shown in Figure 4(a) that when the reduced-order perturbation gets close to the original perturbation, the error of reduced-order model with respect to the exact is always less than 40 Hz, which is also a satisfactory result. The same is for frequencies 29 and 30 when choosing $\Gamma^* = \{29, 30, 32\}$; as is shown in Figure 4(b), there is hardly any error between the result of reduced-order model and the exact.

Obviously, this reduced-order model is so effective that it can be used to the critical coefficient of friction that means the onset of squeal as well as the squeal frequency with sufficient accuracy and largely reduced amount of calculation, thus giving us a practical guide to perform design optimization in order to reduce brake squeal.

5. Conclusions

Brake squeal is often analytically studied by a complex eigenvalue analysis of linearized models of the brake assembly that is usually quite large. In this paper, a time-saving method for determining those frequencies having the most effect on the pair of coupling frequencies is put forward and a reduced-order model is presented based on the complex modes theory.

The method for determining the influential set is efficient, which only needs to solve the eigenvalues and their derivatives for the unperturbed system and the reduced-order system. The reduced-order model gives good estimations of

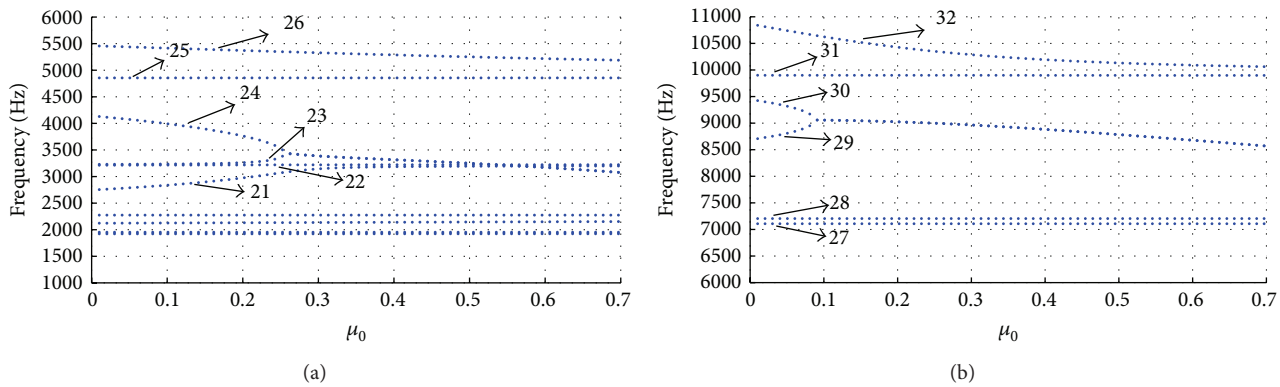

FIGURE 2: Evolution of the frequency versus μ_0 (a) in the frequency range of 1–6 kHz (b) in the frequency range of 6–11 kHz. Fixed parameters: $K = 8 \times 10^8$ N/m, $r_0 = 0.09$ m, $\gamma = 5^\circ$, $\Omega = 20$ rad/s, $S_1 = 0$, and $D^* = c_t = c_a = 0$.

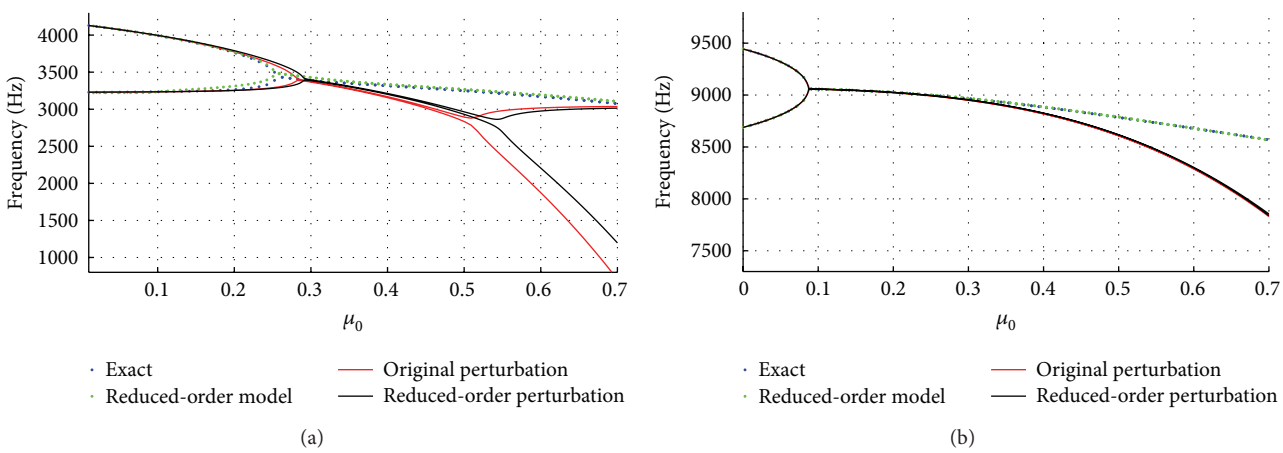

FIGURE 3: Comparison between the frequencies versus μ_0 of original model with those of reduced-order model (a) in the frequency range of 0.8–4.3 kHz and (b) in the frequency range of 7.3–9.8 kHz. Blue points—exact frequencies; green points—frequencies of reduced-order model; red line—original perturbation frequency locus; black line—reduced-order perturbation frequency locus. Fixed parameters: $K = 8\times10^8$ N/m, $r_0 = 0.09$ m, $\gamma = 5^\circ$, $\Omega = 20$ rad/s, $S_1 = 0$, $D^* = c_t = c_a = 0$, and $M = 5$.

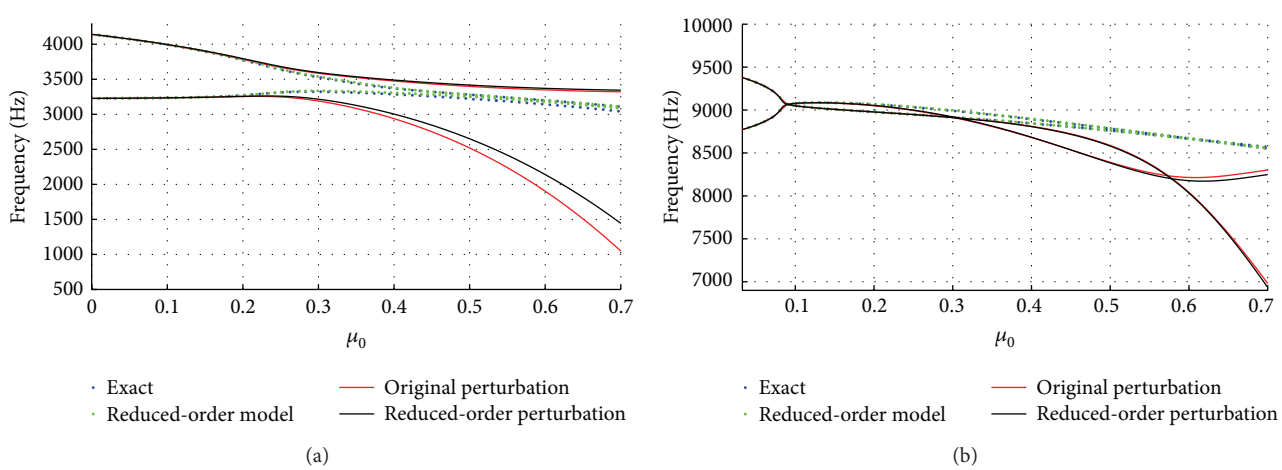

FIGURE 4: Comparison between the frequencies versus μ_0 of original model with those of reduced-order model (a) in the frequency range of 0.5–4.3 kHz and (b) in the frequency range of 6.9–10 kHz. Blue points—exact frequencies; green points—frequencies of reduced-order model; red line—original perturbation frequency locus; black line—reduced-order perturbation frequency locus. Fixed parameters: $K = 8\times10^8$ N/m, $r_0 = 0.09$ m, $\gamma = 5^\circ$, $\Omega = 20$ rad/s, $S_1 = -0.1$ s/m, $D^* = c_t = c_a = 0.05$ N · s/m, and $M = 5$.

the exact result when the influential set is determined and is proved to be effective when applied to a flexible pin-on-disc system, even damping and nonlinearity are taken into consideration.

This reduce-order model can predict the onset of squeal as well as the squeal frequency with sufficient accuracy and largely reduced amount of calculation and gives us a practical guide to perform design optimization in order to reduce brake squeal.

Appendix

Consider

$$\begin{aligned}
\mathbf{y} &= \left(x_{kl}, p_n^t(t), p_n^a(t)\right)^T, \\
\mathbf{C} &= \operatorname{diag}[l, 0 \cdots 0], \\
\mathbf{D} &= \mathbf{C}^2, \\
\mathbf{C}_s &= 2\operatorname{diag}\left[\xi_{kl}\omega_{kl}, \xi_n^t\omega_n^t, \xi_n^a\omega_n^a\right], \\
\left[\omega^2\right] &= \operatorname{diag}\left[\omega_{kl}^2, \omega_n^{t2}, \omega_n^{a2}\right], \\
\mathbf{R}_A &= \left(R_{kl}(r_0), \varphi_n^t(l)\sin\gamma, -\varphi_n^a(l)\cos\gamma\right), \\
\mathbf{R}_C &= \left(0 \cdots 0, \varphi_n^t(l)\cos\gamma, \varphi_n^a(l)\sin\gamma\right), \\
\mathbf{R}_B &= -\frac{jh}{2r_0}\mathbf{R}_A\mathbf{C} + \mathbf{R}_C, \\
\mathbf{A} &= \mathbf{R}_A^T\mathbf{R}_A, \\
\mathbf{B} &= -\mathbf{R}_B^T\mathbf{R}_A = \left(\frac{jh}{2r_0}\mathbf{R}_A\mathbf{C} - \mathbf{R}_C\right)^T\mathbf{R}_A \\
&= \frac{jh}{2r_0}\mathbf{C}\mathbf{A} - \mathbf{R}_C^T\mathbf{R}_A \\
&(k = 0, 1, 2, \ldots;\ l = 0, \pm1, \pm2, \ldots,\ n = 1, 2, \ldots).
\end{aligned} \tag{A.1}$$

Nomenclature

Variables

a, b:	Inner and outer radius of the disc
c_t, c_a:	Kelvin-type damping coefficient of the pin in the transverse and axial direction
d:	The diameter of cross-sectional area of the pin
D:	Flexible rigidity of the disc
D^*:	Kelvin-type damping coefficient of the disc
E_d, E_p:	Young's modulus of the disc and pin material
F_f:	The friction force acting on the pin
F_L:	Preload between the pin and disc
F_N:	The normal force acting on the pin
h:	Thickness of the disc
I:	Second moment of the cross-sectional area of the pin
K:	Contact stiffness between the pin and disc
l:	The length of the pin
r:	Radial coordinate in the cylindrical coordinate system
S:	Cross-sectional area of the pin
t:	Time
$u^a(x,t)$:	Axial displacement of the pin
$u^t(x,t)$:	Transverse displacement of the pin
$w(r,\theta,t)$:	Out-of-plane displacement of the disc
γ:	Angle of inclination of the pin
θ:	Circumferential coordinate in the cylindrical coordinate system
μ:	Coefficient of friction
ν_d, ν_p:	Poisson's ratio of the disc and pin
ρ_d, ρ_p:	Density of the disc and pin
Ω:	Rotational speed of the disc.

Conflict of Interests

The authors declare that there is no conflict of interests regarding the publication of this paper.

Acknowledgments

This research is sponsored by the National Natural Science Foundation of China (NSFC), Grant no. 51175380. The authors greatly appreciate the support provided by NSFC during this research.

References

[1] N. M. Kinkaid, O. M. O'Reilly, and P. Papadopoulos, "Automotive disc brake squeal," *Journal of Sound and Vibration*, vol. 267, no. 1, pp. 105–166, 2003.

[2] F. Massi and O. Giannini, "Extension of a modal instability theory to real brake system," in *Proceedings of the International Modal Analysis Conference (IMAC '05)*, 2005.

[3] M. R. North, "Disc brake squeal, a theoretical model," Tech. Rep. 1972/5, Motor Industry Research Association, Warwickshire, UK, 1972.

[4] A. Akay, J. Wickert, and Z. Xu, "Investigation of mode lock-in and friction interface," Final Report, Department of Mechanical Engeneering, Carnegie Mellon University, Pittsburgh, Pa, USA, 2000.

[5] J. Flint and J. Hultén, "Lining-deformation-induced modal coupling as squeal generator in a distributed parameter disc brake model," *Journal of Sound and Vibration*, vol. 254, no. 1, pp. 1–21, 2002.

[6] J. Huang, C. M. Krousgrill, and A. K. Bajaj, "An efficient approach to estimate critical value of friction coefficient in brake squeal analysis," *Journal of Applied Mechanics*, vol. 74, no. 3, pp. 534–541, 2007.

[7] H. Ouyang, L. Baeza, and S. Hu, "A receptance-based method for predicting latent roots and critical points in friction-induced vibration problems of asymmetric systems," *Journal of Sound and Vibration*, vol. 321, no. 3–5, pp. 1058–1068, 2009.

[8] C. Chung, W. Steed, K. Kobayashi, and H. Nakata, "A new analysis method for brake squeal part I: theory for modal domain formulation and stability analysis," SAE Paper 2001-01-1600, 2001.

[9] J. Huang, C. M. Krousgrill, and A. K. Bajaj, "Modeling of automotive drum brakes for squeal and parameter sensitivity analysis," *Journal of Sound and Vibration*, vol. 289, no. 1-2, pp. 245–263, 2006.

[10] J. Kang, C. M. Krousgrill, and F. Sadeghi, "Analytical formulation of mode-coupling instability in disc-pad coupled system," *International Journal of Mechanical Sciences*, vol. 51, no. 1, pp. 52–63, 2009.

[11] C. Suhuan, *Matrix Perturbation Theory in Structural Dynamic Design*, Science Press, Beijing, China, 2007.

[12] D. Hochlenert, G. Spelsberg-Korspeter, and P. Hagedorn, "Friction induced vibrations in moving continua and their application to brake squeal," *Journal of Applied Mechanics*, vol. 74, no. 3, pp. 542–549, 2007.

[13] H. Ouyang and J. E. Mottershead, "Dynamic instability of an elastic disk under the action of a rotating friction couple," *Journal of Applied Mechanics*, vol. 71, no. 6, pp. 753–758, 2004.

[14] H. Hetzler, D. Schwarzer, and W. Seemann, "Analytical investigation of steady-state stability and Hopf-bifurcations occurring in sliding friction oscillators with application to low-frequency disc brake noise," *Communications in Nonlinear Science and Numerical Simulation*, vol. 12, no. 1, pp. 83–99, 2007.